

New Heterogeneous Nano-Catalyst: Synthesis and Catalytic Effect on the Green Synthesis of 1-Substituted and 5-Substituted 1H-Tetrazole Derivatives

Mahboobeh-Sadat Mashhoori (✉ m.mashhoori2015@birjand.ac.ir)

University of Birjand

Reza Sandaroots

University of Birjand

Research Article

Keywords:

Posted Date: March 7th, 2022

DOI: <https://doi.org/10.21203/rs.3.rs-1356738/v1>

License: © ⓘ This work is licensed under a Creative Commons Attribution 4.0 International License.

[Read Full License](#)

Abstract

A novel heterogeneous catalyst containing Schiff base coordinated Cu(II) covalently attached to Fe₃O₄@SiO₂ nanoparticles through imidazolium linker [Fe₃O₄@SiO₂-Im(Br)-SB-Cu (II)] was synthesized and characterized by using various techniques. The catalytic efficiency of this nano-catalyst was tested in the synthesis of tetrazole derivatives. The investigation revealed that i) The catalyst is very efficient in the synthesis of tetrazole derivatives with high yield (97%) in aqueous medium; ii) The catalytic effectiveness is due the synergy between the metallic center and the imidazolium ion and iii) The reuse advantage of the catalyst without contamination or significant loss (12% of loss range) in the catalytic activity.

Introduction

Tetrazoles are essential class of poly-aza-heterocyclic compounds largely discovered in nature.¹ Recently, tetrazoles have received much attention due to their large spectrum of applications in the field of medicine and biology such as anticancer, antiviral, antiallergic, antibiotic, anti-HIV, etc.,²⁻⁵ Homogeneous catalysts were predominantly used, due to their solubility and high activity, in the synthesis of tetrazole derivatives than their heterogeneous counterparts. However, homogeneous catalysts suffer from many drawbacks such as high-temperature working conditions, difficult recycling, product contamination, and deactivation through dimerization. To overcome these problems, methods were devised to heterogenize such catalysts, including polymerization^{7,8}, grafting them on organic⁹ or inorganic supports^{10,11,12}. One of the best solid support is magnetic nanoparticles, especially Fe₃O₄, due to several factors such as high active surface area, low toxicity, superparamagnetism,¹³ ease of recycling,^{14,15} high dispersion and reactivity, and chemical/thermal stability. Also, ease of surface modification and ligands coupling due to the chemical nature and accessible reactive groups on the surface of the nanoparticles.²⁴

Our strategy was to design and synthesize a heterogeneous catalyst that is suitable to work in aqueous conditions. To allow the catalyst to work in water, our design approach was based on the use of water-soluble linker or coupling spacer arm to bring the catalyst to aqueous medium during the catalytic process. We decided to prepare a Cu(II)-coordinated Schiff base nano-catalyst having an imidazolium linker to nanoparticles. The nano-catalyst efficiency was then successfully investigated in tetrazole derivatives synthesis in aqueous medium. The catalyst achieved high tetrazole derivatives yield in a short reaction time and, due to its magnetic characteristic, it was easily removed from the products without leaving behind any metallic contamination.

Experimental

Materials and apparatus

All solvents were purchased from Merck Co. and dried by standard procedures. All chemical reagents were purchased from Sigma-Aldrich chemical company and used without further purification. The

progress of reactions was monitored by TLC on Silica-gel Polygram SILG/UV254 plates. Fourier Transform Infrared (FT-IR) spectra were recorded on a PerkinElmer 780 FT-IR spectrometer (KBr tablets). The morphology (SEM) and elemental analysis (EDS) of the catalyst were determined by using the FE-SEM TESCAN MIRA3 instrument. Transmission Electron Microscopy (TEM) images were obtained with a Philips EM208 S electron microscope. X-ray Diffraction (XRD) patterns were collected using a Philips PW 1730 diffractometer using Cu K α radiation ($\lambda = 1.54 \text{ \AA}$). Thermogravimetric Analysis (TGA) was performed on a Q600 TA instrument at 30–700 °C with a heating rate of 20 °C min⁻¹ in an argon atmosphere. Vibrating Sample Magnetometer (VSM) analysis was performed at room temperature using an LBKFB instrument. Inductively Coupled Plasma-Optical Emission Spectroscopy (ICP-OES) analysis was performed using a Simultaneous VISTA-PRO instrument. Atomic Absorption Spectroscopy (AAS) analysis was performed using a Shimadzu AA6200 instrument.

The synthesis of modified silica coated Fe₃O₄ nanoparticles (Fe₃O₄@SiO₂)

The silica coated Fe₃O₄ magnetic nanoparticles were synthesized by previously reported methods.²⁶ FeCl₃·6H₂O (6.8 g) and FeCl₂·4H₂O (2.5 g) were added to deionized water (300 mL) and stirred under nitrogen gas at room temperature. Gradually, ammonia solution (25% w/w, 70 mL) was added to the vigorously stirred mixture. As soon as the solution's color turned black, the resulting nanoparticles were separated by an external magnet and washed several times with deionized water.

To synthesize silica-coated nanoparticles, Fe₃O₄ nanoparticles (3.0 g) were dispersed by sonication in a deionized water/ethanol solvent mixture (1:4 v/v, 500 mL) 30 minutes. Then a solution of ammonia (25% w/w) was gradually added until the pH reaches 10. The tetraethyl orthosilicate (TEOS, 20 mL) was slowly added to the mixture and stirred three hours at 50 °C. The silica-coated nanoparticles (Fe₃O₄@SiO₂) were collected by a permanent magnet and washed with deionized water and ethanol several times and dried in a vacuum oven at 50 °C for 24 hrs. In the final stage, Fe₃O₄@SiO₂ (1g) was sonicated in dry toluene (40 mL) for 30 min. Then, 3-Chloropropyl triethoxysilane (2.0 mL) was added dropwise and refluxed for 20 hours. The resulting chloro-modified Fe₃O₄@SiO₂ was removed from the reaction mixture by a strong magnet, washed with in toluene, ethanol and diethyl ether for several times. Then dried under vacuum at 60 °C for 12hrs.²⁷ The loading amount of Cl atom was 0.3 mmol per gram catalyst based on EDX.

The synthesis of Fe₃O₄@ SiO₂-Im nanoparticles

Imidazole (0.5 mmol, 0.034 g) was added to the dispersed solution of chloro-modified Fe₃O₄@SiO₂ (1.0 g) in dry toluene (40 mL) and triethylamine (NEt₃, 0.5 mmol, 0.05 g) was added dropwise and refluxed for 24 hrs. The resulting nanoparticles were separated with the external magnet and washed with distilled water and ethanol. The resulted Fe₃O₄@ SiO₂-Im nanoparticles were dried in a vacuum oven at 80 °C for 12hrs.

The synthesis of Fe₃O₄@ SiO₂-Im[Br] nanoparticles

The synthesized nanoparticles of $\text{Fe}_3\text{O}_4@\text{SiO}_2\text{-Im}$ (1.0 g) in dry ethanol (40 mL) were dispersed for 30 mins by sonication. The ethanolic solution of 3-Bromopropylamin hydrobromide (0.5 mmol, 0.11 g) was gradually added to the stirred mixture and refluxed for 48 hours. The resulting nanoparticles were separated by the magnet, washed with distilled water, ethanol, and diethyl ether. Finally, nanoparticles were dried in a vacuum at 80 °C for 20 hrs.

The synthesis of $\text{Fe}_3\text{O}_4@\text{SiO}_2\text{-Im[Br]-SB}$ nanoparticles

The nanoparticles ($\text{Fe}_3\text{O}_4@\text{SiO}_2\text{-Im [Br]-PrNH}_2$. HBr, 1.0 g) from the previous step were dispersed by sonication in dry ethanol (40 mL) followed by dropwise addition of salicylaldehyde (0.5 mmol, 56 μL) and sodium hydroxide (NaOH, 0.5 mmol, 0.02 g) solutions. The reaction mixture was then refluxed in ethanol 20 hours. The resulting nanoparticles were separated by the magnet and washed with distilled water, ethanol, and diethyl ether. Finally, nanoparticles were dried in a vacuum at 80 °C for 20 hrs.

The synthesis of $\text{Fe}_3\text{O}_4@\text{SiO}_2\text{-Im[Br]-SB-Cu (II)}$ Nano-complex

The ethanolic solution of $\text{Cu (OAc)}_2 \cdot \text{H}_2\text{O}$ (0.8 mmol, 0.16 g) was added dropwise to the well dispersed $\text{Fe}_3\text{O}_4@\text{SiO}_2\text{-Im [Br]-Schiff}$ base nanoparticles (1.0 g) in ethanol and refluxed 12 hrs. The resulting Cu(II)-coordinated nanoparticles were separated by an external magnet and washed several times with ethanol, diethyl ether and dried in a vacuum at 60 °C for 10 hrs.

General procedure for the synthesis of 1-substituted 1H-tetrazole

aniline (1.0 mmol, 0.09 mL), Triethyl orthoformate (1.2 mmol, 0.2 mL), sodium azide (1.0 mmol, 0.06 g) in a water (1.0 mL) in the presence of $\text{Fe}_3\text{O}_4@\text{SiO}_2\text{-Im[Br]-SB-Cu (II)}$ nano-catalyst (0.6 mol%, 0.008 g) were stirred at 40 °C. The reaction progression was monitored by thin-layer chromatography (TLC) at different interval of time using n-Hexane/Ethyl acetate (4:1) as eluent. At the end, the reaction mixture was cooled, and catalyst removed by an external magnet. The reaction mixture was extracted with 3x10mL of ethyl acetate. The organic phase was dried with anhydrous Na_2SO_4 , filtered and then evaporated. The pure product was obtained by recrystallization in a mixture of n-Hexane/Ethyl acetate. The recovered yield was 97%.

General procedure for the synthesis of 5-substituted 1H-tetrazole

Benzaldehyde (1.0 mmol, 0.1 mL), hydroxylammonium chloride (1.0 mmol, 0.07 g), sodium azide (1.2 mmol, 0.08 g) in water (1.0 mL) in the presence of $\text{Fe}_3\text{O}_4@\text{SiO}_2\text{-Im[Br]-SB-Cu (II)}$ nano-catalyst (0.9 mol%, 0.012 g) were stirred at 40 °C. The reaction was followed by thin-layer chromatography (TLC) at different time intervals in (n-Hexane/Ethyl acetate: 4:1). The reaction mixture was cooled, and the catalyst removed by an external magnet. 5mL of HCl (5 N) was added to the reaction mixture and extracted with 3x10mL of ethyl acetate. The organic phase was extracted again with the HCl solution (1 N), followed by a saturated solution of NaCl. The organic phase was dried with the anhydrous Na_2SO_4 , filtered and then

evaporated. The pure product was obtained in 97% yield by recrystallization with n-Hexane/Ethyl acetate solvent mixture.

Results And Discussion

Catalyst Characterization

$\text{Fe}_3\text{O}_4@\text{SiO}_2\text{-Im[Br]-SB-Cu(II)}$ nano-catalyst was synthesized (Scheme 1) and investigated in the synthesis of tetrazole derivatives (Scheme 2). The prepared catalyst is characterized by various methods. The FT-IR spectra of the catalyst synthesis steps are shown in Fig. 1. The spectrum 1a, which corresponds to the Fe_3O_4 nanoparticles, show the peaks at 571 and 3442 cm^{-1} corresponding to stretching vibrations of Fe-O and OH groups, respectively.^{28,29} The appearance of new picks at 1077 and 1192 cm^{-1} are corresponding to Si-O (Symm.) and Si-O (Asymm.), respectively. These picks are a confirmation that the surface of nanoparticles is protected by silica coating layer (Fig. 1, 1b).³⁰ The transmittance of core shelled Fe_3O_4 nanoparticles was slightly lower than that of Fe_3O_4 nanoparticles due to silica coating. Absorbed picks in 2852 (Symm.), 2934 (Asymm.), 1420 (Bending) and 814 cm^{-1} , respectively, correspond to CH_2 and C-Cl are evidence of the modification of nanoparticles surface (Fig. 1, 1c).³¹ The disappearing C-Cl pick and the appearance of new picks in 1632 and 1742 cm^{-1} indicate that the imidazole ring was coupled to the nanoparticles surface (Fig. 1, 1d).³² The spectrum 1e shows pick in 3422 cm^{-1} , which correspond to NH of amine group. The new pick at 1636 cm^{-1} is evidence of the formation of imine (Fig. 1, 1f).³³ The new picks at 635 and 620 cm^{-1} correspond to Cu-N and Cu-O. Also, the transfer of imine peak to lower frequencies confirms the formation of the metal complex (Fig. 1, 1g).

The elemental composition of $\text{Fe}_3\text{O}_4@\text{SiO}_2\text{-Cl}$ (Fig. 2) and the nano-catalyst $\text{Fe}_3\text{O}_4@\text{SiO}_2\text{-Im[Br]-SB-Cu (II)}$ (Fig. 3) was estimated by Energy Dispersive X-rays (EDX) analysis. Absence of chlorine element in the nano-catalyst confirms the attachment of ionic metal Schiff base complex on the surface of modified nanoparticles leading to the nano-catalyst. Anticipated elemental composition: C (10.40%), N (3.77%), O (40.21%), Si (5.48%), Fe (36.49%), Br (0.57%) and Cu (3.10%).

The morphology of $\text{Fe}_3\text{O}_4@\text{SiO}_2\text{-Im[Br]-SB-Cu (II)}$ nano-catalyst was determined by Scanning Electron Microscopy (SEM). SEM images show spherical and irregular shapes for the nanoparticles (Fig. 4).

The X-ray diffraction (XRD) patterns of Fe_3O_4 , $\text{Fe}_3\text{O}_4 @ \text{SiO}_2$ and $\text{Fe}_3\text{O}_4@\text{SiO}_2\text{-Im [Br] -SB-Cu (II)}$ are shown in Fig. 5. The XRD pattern of Fe_3O_4 magnetic nanoparticles is in accordance with (PDF # 88-0866, reference JCPDS card no. 19-629), which shows a crystalline cubic spinel structure.³⁴ XRD patterns of Fe_3O_4 , $\text{Fe}_3\text{O}_4 @ \text{SiO}_2$ and $\text{Fe}_3\text{O}_4 @ \text{SiO}_2\text{-Im[Br]-SB-Cu (II)}$ show the peaks in $2\theta = 30.1^\circ$, 35.4° , 43.1° , 53.4° , 57° , and 62.6° which are related to the pages of (220), (311), (400), (422), (511), and (440), respectively and are in full agreement with the Fe_3O_4 pattern showing that their crystalline phase and position have not changed. These results indicate that the crystalline cubic structure of nanoparticles

Fe_3O_4 is preserved during the catalyst preparation process. In the $\text{Fe}_3\text{O}_4@\text{SiO}_2$ spectrum, a broad peak is observed in $2\theta = 10\text{--}20^\circ$, which is related to amorphous silica. This broad peak for the nano-catalyst was shifted to lower angles due to the synergetic effect of amorphous silica and Cu(II)-coordinated Schiff base. The average size of nanoparticles was calculated by the Debye–Scherrer equation ($D = K.\lambda / \beta.\cos\theta$, λ (wavelength, 0.154 nm), K (a crystallized form factor, 0.94), β (Full width at half maximum, (rad)), θ (Bragg reflection angle, ($^\circ$))) to be about 28 nm which correspond to the TEM results.

The magnetic property of nano-catalyst was measured at different steps of the synthesis by vibrating sample magnetometer (VSM) (Fig. 6). As shown in Fig. 6, the magnetic properties of nanoparticles are gradually reduced by the silica layer coating and the by the coupling of the Cu(II)-complex to the surface of the nanoparticles. Although the magnetic saturation values for Fe_3O_4 , $\text{Fe}_3\text{O}_4@\text{SiO}_2$ and $\text{Fe}_3\text{O}_4@\text{SiO}_2\text{-Im[Br]-SB-Cu (II)}$ are 80, 58 and 38 emu g^{-1} , respectively, nano-catalyst has still a strong magnetic property for its removal from the reaction mixture by an external magnet.

The thermal stability of $\text{Fe}_3\text{O}_4@\text{SiO}_2\text{-Im[Br]-SB-Cu (II)}$ nano-catalyst was examined by TGA technique (Fig. 7). In the thermogram diagram of this catalyst, the maximum weight loss occurs in the range of 414 to 500 $^\circ\text{C}$ (15%), which is related to removing organic groups from the surface of the catalyst. The two weight losses before 414 $^\circ\text{C}$ and 138 $^\circ\text{C}$, are related to removing hydroxyl groups (5%) and adsorbed water molecules on the surface of iron oxide nanoparticles, respectively. Based on this graph and the ICP-OES analysis, the ligand to metal ratio was estimated to be 2: 1.

The amount of supported copper on the $\text{Fe}_3\text{O}_4@\text{SiO}_2\text{-Im[Br]-SB-Cu (II)}$ nano-catalyst was determined by AAS & ICP-OES analyzes. AAS analysis showed 0.83 mmol/g of Cu (II) on the nano-catalyst surface. This Cu(II) content was confirmed by the ICP-OES analysis which showed a 0.72 mmol of Cu(II) per gram of nano-catalyst.

The catalytic activity of $\text{Fe}_3\text{O}_4@\text{SiO}_2\text{-Im[Br]-SB-Cu (II)}$ was investigated in the synthesis of 1-phenyl and 5-phenyl 1-H tetrazole derivatives. The synthesis of 1-phenyl 1-H tetrazole derivatives was optimized using the reaction model of aniline, triethyl orthoformate, and sodium azide (Scheme 3). The results of this investigation are summarized in Table 1. Firstly, the reaction efficiency in polar solvents is higher than in non-polar solvents (Entries 1–8). This is probably due to the ionic nature of catalyst. The reaction was run in the presence of different level of catalyst and the best result was obtained with 0.6 mol% of catalyst. A control reaction with 0 mol% of catalyst was run and as expected no product was obtained (Entry 9). Other reactions controls were tried in the presence of Fe_3O_4 and $\text{Fe}_3\text{O}_4@\text{SiO}_2\text{-Im[Br]}$ (Entries 14, 15) with very low efficiency. The effect of the temperature and time on the reaction were also investigated (Entries 16–21) and we concluded that the best conditions are: H_2O solvent, 0.6 mol% of the catalyst loading, time 20 min and 40 $^\circ\text{C}$.

The synthesis of 1-phenyl 1-H tetrazole derivatives

Table 1
Optimization of the reaction conditions for the synthesis of 1-phenyl- 1H tetrazole derivatives

Entry	Solvent	Catalyst (mol %)	Temperature (°C)	Time (min)	Yield (%) ^b	TON ^c	TOF (h ⁻¹) ^d
1	H ₂ O	0.6	40	20	97	162	486
2	MeOH	0.6	40	20	75	125	375
3	EtOH	0.6	40	20	70	117	9.8
4	THF	0.6	40	20	30	50	150
5	CH ₃ CN	0.6	40	20	60	67	201
6	CHCl ₃	0.6	40	20	40	67	201
7	CH ₂ Cl ₂	0.6	40	20	40	80	240
8	Solvent-free	0.6	40	20	85	142	426
9	H ₂ O	-	40	24 h	-	-	-
10	H ₂ O	0.4	40	20	80	133	399
11	H ₂ O	0.9	40	20	90	150	450
12	H ₂ O	1	40	20	85	142	426
13	H ₂ O	1.4	40	20	78	130	390
14 ^e	H ₂ O	0.008 gr	40	24 h	30	50	2.08
15 ^f	H ₂ O	0.008 gr	40	24 h	50	83	3.5
16	H ₂ O	0.6	rt	20	60	100	300
17	H ₂ O	0.6	60	20	95	158	474
18	H ₂ O	0.6	80	20	85	142	426
19	H ₂ O	0.6	100	20	70	117	351
20	H ₂ O	0.6	40	10	70	117	702
21	H ₂ O	0.6	40	30	92	153	306

a Aniline (1.0 mmol), Triethyl orthoformate (1.2 mmol), Sodium azide (1mmol) and Fe₃O₄@SiO₂-Im[Br]-SB-Cu (II).

Entry	Solvent	Catalyst (mol %)	Temperature (°C)	Time (min)	Yield (%) ^b	TON ^c	TOF (h ⁻¹) ^d
^b Isolated yield.							
^c Turnover numbers (TONs) defined as mmol of products reacted per mmol of catalyst.							
^d Turnover frequencies (TOFs) defined as mmol of products reacted per mmol of catalyst per hour.							
^e Fe ₃ O ₄ (0.008 gr).							
^f Fe ₃ O ₄ @SiO ₂ -Im[Br] (0.008 gr)							

After optimizing the reaction conditions, different 1-phenyl 1H-tetrazole derivatives were synthesized by using different aniline derivatives under the same conditions (Table 2). The reaction in the presence of electron-donating and electron-withdrawing groups on benzaldehyde and the spatial barrier on aniline have significant impact on the reaction efficacy (Entries 2, 3 & 7, 8).

Table 2. Synthesis of 1-phenyl-1H-tetrazole derivatives in the presence Fe₃O₄@SiO₂-Im[Br]-SB-Cu (II) catalyst^a

Entry	R	Product	Time (min)	Yield (%) ^b	MP found (Lit.) (°C) [34]
1	H	4a	20	97	64–66 (64–65)
2	2-Cl	4b	30	86	127–130 (127–131)
3	4-Cl	4c	30	95	156–158 (157–158)
4	4-CH ₃	4d	15	92	92–94 (94–95)
5	4-OCH ₃	4e	10	92	115–117 (114–115)
6	4-NO ₂	4f	60	92	200–204 (201–202)
7	2-OH	4g	45	90	205–207 (-)
8	4-OH	4h	15	95	215–218 (-)
9	4-Br	4i	30	90	181–184 (183–185)

^a Reaction conditions: Aniline (1.0 mmol), Triethyl orthoformate (1.2 mmol), Sodium azide (1.0 mmol) and Fe₃O₄@SiO₂-Im[Br]-SB-Cu (II) (0.5 mol %) in the water at 40 °C.

^b Isolated yield.

The plausible mechanism for the synthesis of 1-phenyl- 1H tetrazole derivatives by using $\text{Fe}_3\text{O}_4@\text{SiO}_2@\text{Im}[\text{Br}]\text{-SB-Cu (II)}$ nano-catalyst is depicted in Scheme 4.³⁶

The reaction model using benzaldehyde, hydroxy amine hydrochloride and sodium azide was selected to optimize the conditions for the synthesis of 5-phenyl- 1H-tetrazole derivatives (Scheme 5). The results of this investigation are shown in Table 3. Firstly, water was identified as the solvent of choice (Entries 1–8). As in the case of 5-phenyl 1-H tetrazole derivatives, we confirmed that the reaction needs the catalyst to proceed and no product was obtained in the absence of the catalyst (Entries 9–13). In this reaction model, the highest conversion rate was obtained in the presence of 0.9 mol% of catalyst (Entry 1). Also in the presence of the precursor of our catalyst (Fe_3O_4 and $\text{Fe}_3\text{O}_4@\text{SiO}_2\text{-Im}[\text{Br}]$), the reaction conversion rate was very low (Entries 14, 15). The effect of temperature and reaction time was also investigated (Entries 16–21) and the best conditions are: H_2O as solvent, 0.9 mol% of the catalyst, time 20 min and 40°C .

Table 3

Optimization of the reaction conditions for the synthesis of 5-phenyl- 1H tetrazole derivatives ^a

Entry	Solvent	Catalyst (mol %)	Temperature (°C)	Time (min)	Yield (%) ^b	TON ^c	TOF ^d
1	H ₂ O	0.9	40	20	97	108	323
2	MeOH	0.9	40	20	80	88.9	267
3	EtOH	0.9	40	20	70	77.8	233
4	THF	0.9	40	20	20	22.2	66.6
5	CH ₃ CN	0.9	40	20	40	44.4	133.3
6	CHCl ₃	0.9	40	20	30	33.3	100
7	CH ₂ Cl ₂	0.9	40	20	30	33.3	
8	Solvent-free	0.9	40	20	70	77.8	233
9	H ₂ O	-	40	24 h	-	-	-
10	H ₂ O	0.4	40	20	70	140	420
11	H ₂ O	0.6	40	20	85	94	282
12	H ₂ O	1	40	20	90	100	300
13	H ₂ O	1.4	40	20	75	83	249
14 ^e	H ₂ O	0.9	40	24 h	30	33.3	1.4
15 ^f	H ₂ O	0.9	40	24 h	50	55.5	2.3
16	H ₂ O	0.9	rt	20	60	66.6	200

^a Benzaldehyde (1.0 mmol), hydroxy amine hydrochloride (1.0 mmol), Sodium azide (1.2 mmol) and Fe₃O₄@SiO₂-Im[Br]-SB-Cu (II) (0.9 mol%, 0.012 g).

^b Isolated Yield.

^c Turnover numbers (TONs) defined as mmol of products reacted per mmol of catalyst.

^d Turnover frequencies (TOFs) defined as mmol of products reacted per mmol of catalyst per hour.

^e Fe₃O₄ (0.012 gr).

^f Fe₃O₄@SiO₂-Im[Br] (0.012 gr).

Entry	Solvent	Catalyst (mol %)	Temperature (°C)	Time (min)	Yield (%) ^b	TON ^c	TOF ^d
17	H ₂ O	0.9	60	20	97	108	323
18	H ₂ O	0.9	80	20	85	94.4	283
19	H ₂ O	0.9	100	20	75	83.3	250
20	H ₂ O	0.9	40	10	75	83	498
21	H ₂ O	0.9	40	30	90	100	200
^a Benzaldehyde (1.0 mmol), hydroxy amine hydrochloride (1.0 mmol), Sodium azide (1.2 mmol) and Fe ₃ O ₄ @SiO ₂ -Im[Br]-SB-Cu (II) (0.9 mol%, 0.012 g).							
^b Isolated Yield.							
^c Turnover numbers (TONs) defined as mmol of products reacted per mmol of catalyst.							
^d Turnover frequencies (TOFs) defined as mmol of products reacted per mmol of catalyst per hour.							
^e Fe ₃ O ₄ (0.012 gr).							
^f Fe ₃ O ₄ @SiO ₂ -Im[Br] (0.012 gr).							

Different 5-phenyl 1H-tetrazole derivatives were synthesized using different benzaldehyde derivatives under the optimized conditions (Table 4). The results show that the reaction efficiency is impacted by the electronic properties and the position of the substituents groups on the benzaldehyde ring.

Table 4. Synthesis of 5-Phenyl-1H-Tetrazole derivatives in presence of Fe₃O₄@SiO₂-Im[Br]-SB-Cu (II) catalyst ^a

Entry	R	Product	Time (min)	Yield (%)	MP Found (Lit.) (°C)
1	H	4a	20	97	214–216 (215–216) [36]
2	2-Cl	4b	45	80	230–233 (-)
3	4-Cl	4c	20	80	260–262 (261–263) [37]
4	4-CH ₃	4d	20	82	253–254 (250–251) [41]
5	4-OCH ₃	4e	20	86	232–234 (231–232) [38]
6	4-NO ₂	4f	60	75	218–220 (218–219) [36]
7	2-OH	4g	30	82	221–223 (220–222) [39]
8	4-OH	4h	20	90	235–236 (233–234) [40]
9	4-Br	4i	20	92	264–266 (265) [42]
Reaction conditions: Benzaldehyde (1.0 mmol), hydroxy amine hydrochloride (1.0 mmol), Sodium azide (1.2 mmol) and Fe ₃ O ₄ @SiO ₂ -Im[Br]-SB-Cu (II) (0.9 mol %, 0.012 g) in water at 40 °C.					
^b Isolated yield.					

The hypothetical mechanism for the formation of 5-phenyl- 1H-tetrazole derivatives using Fe₃O₄@SiO₂-Im[Br]-SB-Cu (II) nano-catalyst is illustrated in Scheme 6.⁴⁴

We studied the reusability of Fe₃O₄@SiO₂-Im[Br]-SB-Cu (II) in the synthesis of tetrazole derivatives. After completing the reaction, the catalyst was separated by an external magnet from the reaction mixture, washed with ethyl acetate, dried, and reused in subsequent catalytic cycles under the same reaction conditions. The recycled catalyst was successfully reused for eight runs (Fig. 8). The FT-IR comparison of fresh and reused catalysts is shown in Fig. 9 with no change in the catalyst structure.

To investigate the heterogenous nature of our catalyst, the hot filtration test was performed.

A hot filtration test was performed to evaluate the metal leaching rate and assess if the catalytic activity of our catalyst is not due to leached Cu(II) species in the reaction mixture (Fig. 10). In the model reaction for the synthesis of 1-Phenyl- 1H-tetrazole derivatives after the half reaction time in which the reaction conversion rate is 50%, the reaction was stopped and catalyst was removed with an external magnet. The reaction mixture without the catalyst was then allowed to proceed further (60 min). After the separation of catalyst from the reaction mixture, no increase in conversion was observed. This is a strong indication that the catalytic process is taking place only in the presence of the nano-catalyst and confirms the heterogeneity of the catalytic process (Fig. 10). The test also indicate that there is no active copper metal species in the synthesis of tetrazole was leached into the reaction mixture.

Our catalyst was benchmarked against published catalyst for the synthesis of tetrazole derivatives (Table 5). The data in Table 5 show that our catalyst (Entry 7) is more efficient than the other reported

catalysts in terms of yield and reaction time.

Table 5
Comparison of $\text{Fe}_3\text{O}_4@\text{SiO}_2\text{-Im[Br]-SB-Cu (II)}$ with other catalysts in synthesis of tetrazole derivatives

Entry	Catalyst	Conditions	Time (min)	Yield (%) ^a	Ref.
1	Cu (OAC)_2	EDS (chcl-urea), 100°C	720	90	[44]
2	$\text{Fe}_3\text{O}_4@\text{WO}_3\text{-EAE-SO}_3\text{H}$	H_2O , 60°C	30	95	[45]
3	Pd-isatin-boehmite	PEG-400, 120°C	480	94	[46]
4	Cu (II) immobilized on $\text{Fe}_3\text{O}_4@\text{SiO}_2@\text{L-Arginine}$	PEG, 120°C	180	95	[47]
5	$\text{Fe}_3\text{O}_4@\text{SiO}_2/\text{Salen Cu (II)}$	DMF, 120°C	420	90	[48]
6	Nano CSMIL ^b	Solvent-free, 70°C	420	87	[49]
7	$\text{Fe}_3\text{O}_4@\text{SiO}_2\text{-Im[Br]-SB-Cu (II)}$	H_2O , 40°C	20	97	This work ^c
^a Isolated Yield.					
^b Chitosan derived magnetic ionic liquid.					
^c Aniline (1.0 mmol), Triethyl orthoformate (1.2 mmol), Sodium azide (1.0 mmol) and $\text{Fe}_3\text{O}_4@\text{SiO}_2\text{-Im[Br]-SB-Cu (II)}$ (0.6 mol %, 0.008 g). Benzaldehyde (1.0 mmol), hydroxy amine hydrochloride (1.0 mmol), Sodium azide (1.2 mmol) and $\text{Fe}_3\text{O}_4@\text{SiO}_2\text{-Im[Br]-SB-Cu (II)}$ (0.9 mol %, 0.012 g).					

Conclusion

A novel and green heterogenous nano-catalyst was prepared. Its catalytic efficiency in water was demonstrated in the synthesis of tetrazole derivatives. This catalyst showed better performance than published catalysts for tetrazole synthesis. The catalyst is easy to recycle with high catalytic efficiency and its intrinsic design allowing for its use in water with high performance may be used as a guidance for the preparation of other useful heterogenous catalytical systems.

Declarations

Acknowledgment

The authors gratefully acknowledge the partial support of this study by the University of Birjand, Birjand, Iran.

Conflicts of interest

There are no conflicts to declare.

Data availability / Availability of Data and Materials

The datasets generated and/or analyzed during the current study are not publicly available due to the continuation of the work at Faculty of Science, University of Birjand, Iran, but are available from the corresponding author on reasonable request.

References

- [1] Sarvary, A. & Maleki, A. A review of syntheses of 1, 5-disubstituted tetrazole derivatives. *Mol. Divers.***19**, 189-212 (2015).
- [2] Sharghi, H., Ebrahimpour moghaddam, S. & Doroodmand, MM. Facile synthesis of 5-substituted-1H-tetrazoles and 1-substituted-1H-tetrazoles catalyzed by recyclable 4'-phenyl-2, 2': 6', 2 "-terpyridine copper (II) complex immobilized onto activated multi-walled carbon nanotubes. *J. Organomet. Chem.* **738**, 41-48 (2013).
- [3] Popova, E.A., Protas, A.V. & Trifonov, R.E. Tetrazole derivatives as promising anticancer agents. *Anti-Cancer Agents Med. Chem.***17**, 1856-1868 (2017).
- [4] Kozikowski, A.P. et al. Synthesis of urea-based inhibitors as active site probes of glutamate carboxypeptidase II: efficacy as analgesic agents. *J. Med. Chem.* **47**, 1729-1738 (2004).
- [5] Mohammad, J. H. Biological activities importance of tetrazole derivatives. *Eur. Acad. Res.***3**, 12803 (2016).
- [6] Corma, A. & Garcia, H. Silica-bound homogenous catalysts as recoverable and reusable catalysts in organic synthesis. *Adv. Synth. Catal.***348**, 1391-1412 (2006).
- [7] Mashhoori, M.S., Sandaroos, R. & Moghaddam, AZ. Polymeric imidazolium ionic liquid-tagged manganese Schiff base complex: An efficient catalyst for the Biginelli reaction. *Res. Chem. Intermed.* **46**, 4939-4954 (2020).
- [8] Mashhoori, M.S., Sandaroos, R. & Zeraatkar Moghaddam, A. Highly Proficient Poly Ionic Liquid Functionalized Mn (III) Schiff-Base Catalyst for Green Synthesis of Chromene Derivatives. *ChemistrySelect.***5**, 7148-7154 (2020).
- [9] Sutar, A. K., Maharana, T., Das, Y. & Rath, P. Polymer supported nickel complex: Synthesis, structure and catalytic application. *J. Chem. Sci.***126**, 1695-1705 (2014).

- [10] Mavrogiorgou, A. & Louloudi, M. Mn-Schiff base modified MCM-41, SBA-15 and CMK-3 NMs as single-site heterogeneous catalysts: Alkene epoxidation with H₂O₂ incorporation. *J. Mol. Catal. A.* **413**, 40-55 (2016).
- [11] Taghizadeh, M. J., Karimi, H. & Sadeghi-Abandansari, H. Vanadium–Schiff base complex-functionalized SBA-15 as a heterogeneous catalyst: synthesis, characterization and application in pharmaceutical sulfoxidation of sulfids. *Res. Chem. Intermed.* **42**, 8201-8215 (2016).
- [12] Godhani, D. R., Nakum, H. D., Parmer, D. K., Mehta, J. P. & Desai, N. C. Tuning of the reaction parameters to optimize allylic oxidation of cyclohexene catalyzed by zeolite-Y entrapped transition metal complexes. *J. Mol. Catal. A*, **415**, 37-55 (2016).
- [13] Lin, Y.S. & Haynes, C.L. Synthesis and characterization of biocompatible and size-tunable multifunctional porous silica nanoparticles. *Chem. Mater.* **21**, 3979-3986 (2009).
- [14] Mondal, J., Sen, T. & Bhaumik, A. Fe₃O₄@ mesoporous SBA-15: a robust and magnetically recoverable catalyst for one-pot synthesis of 3, 4-dihydropyrimidin-2 (1 H)-ones via the Biginelli reaction. *Dalton Trans.***41**, 6173-6181 (2012).
- [15] Gawande, M. B., Branco, P. S. & Varma, R. S. Nano-magnetite (Fe₃O₄) as a support for recyclable catalysts in the development of sustainable methodologies. *Chem. Soc. Rev.***42**, 3371-3393 (2013).
- [16] Tobias, N., Bernhard, S., Heinrich, H., Margarete, H. & Brigitte, V.R. Superparamagnetic nanoparticles for biomedical applications: possibilities and limitations of a new drug delivery system. *J. Magn. Mater.***293**, 483-496 (2005).
- [17] Akira, I. et al. Tumor regression by combined immunotherapy and hyperthermia using magnetic nanoparticles in an experimental subcutaneous murine melanoma. *Cancer Sci.***94**, 308-313 (2003).
- [18] Cai, X., Wang, H., Zhang, Q., Tong, J. & Lei, Z. Magnetically recyclable core–shell Fe₃O₄@ chitosan-Schiff base complexes as efficient catalysts for aerobic oxidation of cyclohexene under mild conditions. *J. Mol. Catal. A.***384**, 217-224 (2014).
- [19] Mohammadikish, M., Masteri-Farahani, M. & Mahdavi, S. Immobilized molybdenum–thiosemicarbazide Schiff base complex on the surface of magnetite nanoparticles as a new nanocatalyst for the epoxidation of olefins. *J. Magn. Mater.***354**, 317-323 (2014).
- [20] Li, X., Fang, Y., Zhou, X., Ma, J. & Li, R. Cobalt (II) acetylacetonate covalently anchored onto magnetic mesoporous silica nanospheres as a catalyst for epoxidation of olefins. *Mater. Chem. Phys.* **156**, 9-15 (2015).
- [21] Ge, Y., Li, Y., Zu, B., Zhou, C. & Dou, X. AM-DMC-AMPS multi-functionalized magnetic nanoparticles for efficient purification of complex multiphase water system. *Nanoscale Res. Lett.* **11**, 1-9 (2016).

- [22] Yoon, H. & Ko, S. Nitrogen-doped magnetic carbon nanoparticles as catalyst supports for efficient recovery and recycling. *J. Jang, Chem. Commun.* 1468-1470 (2007).
- [23] Sheykhan, M., Ma'mani, L., Ebrahimi, A. & Heydari, A. Sulfamic acid heterogenized on hydroxyapatite-encapsulated γ -Fe₂O₃ nanoparticles as a magnetic green interphase catalyst. *J. Mol. Catal. A.* **335**, 253-261 (2011).
- [24] Gawande, M. B., Monga, Y., Zboril, R. & Sharma, R. K. Silica-decorated magnetic nanocomposites for catalytic applications. *Coord. Chem. Rev.* **288**, 118-143 (2015).
- [25] Simon, M.-O. & Li, C.-J. Green chemistry oriented organic synthesis in water. *Chem. Soc. Rev.* **41**, 1415-1427 (2012).
- [26] Pourjavadi, A., Safaie, N., Hosseini, S. H. & Bennett, C. Highly dispersible and magnetically recyclable poly (1-vinyl imidazole) brush coated magnetic nanoparticles: an effective support for the immobilization of palladium nanoparticles. *New J. Chem.* **40**, 1729-1736 (2016).
- [27] Shahbazi, F. & Amani, K. Synthesis, characterization and heterogeneous catalytic activity of diamine-modified silica-coated magnetite-polyoxometalate nanoparticles as a novel magnetically-recoverable nanocatalyst. *Catal. Commun.* **55**, 57-64 (2014).
- [28] Prabhu, Y. T., Rao, K. V., Kumari, B. S., Kumar, V. S. S. & Pavani, T. Synthesis of Fe₃O₄ nanoparticles and its antibacterial application. *Int. Nano Lett.* **5**, 85-92 (2015).
- [29] Esmaeilpour, M., Javidi, J. & Zandi, M. Preparation and characterization of Fe₃O₄@ SiO₂@ PMA: AS an efficient and recyclable nanocatalyst for the synthesis of 1-amidoalkyl-2-naphthols. *Mater. Res. Bull.* **55**, 78-87 (2014).
- [30] Villa, S., Riani, P., Locardi, F. & Canepa, F. Functionalization of Fe₃O₄ NPs by silanization: use of amine (APTES) and thiol (MPTMS) silanes and their physical characterization. *Materials.* **9**, 826 (2016).
- [31] Kazemnejadi, M., Shakeri, A., Mohammadi, M. & Tabefam, M. Direct preparation of oximes and Schiff bases by oxidation of primary benzylic or allylic alcohols in the presence of primary amines using Mn (III) complex of polysalicylaldehyde as an efficient and selective heterogeneous catalyst by molecular oxygen. *J. Iran. Chem. Soc.* **14**, 1917-1933 (2017).
- [32] Wu, Z. et al. Brønsted acidic ionic liquid modified magnetic nanoparticle: an efficient and green catalyst for biodiesel production. *Ind. Eng. Chem. Res.* **53**, 3040-3046 (2014).
- [33] Kazemnejadi, M., Nikookar, M., Mohammadi, M., Shakeri, A. & Esmaeilpour, M. Melamine-Schiff base/manganese complex with dendritic structure: an efficient catalyst for oxidation of alcohols and one-pot synthesis of nitriles. *J. Colloid Interface Sci.* **527**, 298-314 (2018).

- [34] Esmaeilpour, M., Javidi, J., Abarghoui, M. M. & Dodeji, F. N. Synthesis and characterization of $\text{Fe}_3\text{O}_4@ \text{SiO}_2$ -polymer-imid-Pd magnetic porous nanospheres and their application as a novel recyclable catalyst for Sonogashira-Hagihara coupling reactions. *J. Iran. Chem. Soc.* **11**, 499-510 (2014).
- [35] Habibi, D., Nasrollahzadeh, M. & Kamali, T. A. Green synthesis of the 1-substituted 1 H-1,2,3,4-tetrazoles by application of the Natrolite zeolite as a new and reusable heterogeneous catalyst. *Green Chem.* **13**, 3499-3504 (2011).
- [36] Habibi, D. et al. Application of the $\text{Fe}_3\text{O}_4@ 1, 10$ -phenanthroline-5, 6-diol@ Mn nano-catalyst for the green synthesis of tetrazoles and its biological performance. *Appl. Organomet. Chem.* **32**, 4005 (2018).
- [37] Demko, Z.P. & Sharpless, K.B. Preparation of 5-substituted 1 H-tetrazoles from nitriles in water. *J. Org. Chem.* **66**, 7945-7950 (2001).
- [38] Dehghani, F., Sardarian, A. R. & Esmaeilpour, M. Salen complex of Cu (II) supported on superparamagnetic $\text{Fe}_3\text{O}_4@ \text{SiO}_2$ nanoparticles: an efficient and recyclable catalyst for synthesis of 1- and 5-substituted 1H-tetrazoles. *J. Organomet. Chem.* **743**, 87-96 (2013).
- [39] Sreedhar, B., Kumar, A.S. & Yada, D. CuFe_2O_4 nanoparticles: a magnetically recoverable and reusable catalyst for the synthesis of 5-substituted 1H-tetrazoles. *Tetrahedron Lett.* **52**, 3565-3569 (2011).
- [40] Aureggi, V. & Sedelmeier, G. 1, 3-Dipolar cycloaddition: click chemistry for the synthesis of 5-substituted tetrazoles from organoaluminum azides and nitriles. *Angew. Chem. Int. Ed.* **46**, 8440-8444 (2007).
- [41] Esmaeilpour, M., Javidi, J., Nowroozi Dodeji, F. & Mokhtari Abarghoui, M. Facile synthesis of 1-and 5-substituted 1H-tetrazoles catalyzed by recyclable ligand complex of copper (II) supported on superparamagnetic $\text{Fe}_3\text{O}_4@ \text{SiO}_2$ nanoparticles. *J. Mol. Catal. A: Chem.* **393**, 18-29 (2014).
- [42] Jin, T., Kitahara, F., Kamijo, S. & Yamamoto, Y. Copper-catalyzed synthesis of 5-substituted 1H-tetrazoles via the [3+ 2] cycloaddition of nitriles and trimethylsilyl azide. *Tetrahedron Lett.* **49**, 2824-2827 (2008).
- [43] Sardarian, A. R., Eslahi, H. & Esmaeilpour, M. Copper (II) Complex Supported on $\text{Fe}_3\text{O}_4@ \text{SiO}_2$ Coated by Polyvinyl Alcohol as Reusable Nanocatalyst in N-Arylation of Amines and N (H)-Heterocycles and Green Synthesis of 1H-Tetrazoles. *ChemistrySelect.* **3**, 1499-1511 (2018).
- [44] Xiong, X., Yi, C., Liao, X. & Lai, S. A practical multigram-scale method for the green synthesis of 5-substituted-1H-tetrazoles in deep eutectic solvent. *Tetrahedron Lett.* **60**, 402-406 (2019).
- [45] Ghasemzadeh, M. S. & Akhlaghinia, B. 2-Aminoethanesulfonic acid immobilized on epichlorohydrin functionalized $\text{Fe}_3\text{O}_4@ \text{WO}_3$ ($\text{Fe}_3\text{O}_4@ \text{WO}_3$ -EAE- SO_3H): a novel magnetically recyclable heterogeneous

nanocatalyst for the green one-pot synthesis of 1-substituted-1 H-1, 2, 3, 4-tetrazoles in water. *Bull. Chem. Soc. Jpn.* **90**, 1119-1128 (2017).

[46] Jabbari, A., Tahmasbi, B., Nikoorazm, M. & Ghorbani-Choghamarani, A. A new Pd-Schiff-base complex on boehmite nanoparticles: Its application in Suzuki reaction and synthesis of tetrazoles. *Appl Organomet Chem.* **32**, 4295 (2018).

[47] Ghorbani-Choghamarani, A., Shiri, L. & Azadi, G. The first report on the eco-friendly synthesis of 5-substituted 1 H-tetrazoles in PEG catalyzed by Cu (ii) immobilized on Fe₃O₄@SiO₂@ l-arginine as a novel, recyclable and non-corrosive catalyst. *RSC advances.* **6**, 32653-32660 (2016).

[48] Dehghani, F., Sardarian, A. R. & Esmailpour, M. Salen complex of Cu (II) supported on superparamagnetic Fe₃O₄@ SiO₂ nanoparticles: an efficient and recyclable catalyst for synthesis of 1- and 5-substituted 1H-tetrazoles. *J. Organomet. Chem.* **743**, 87-96 (2013).

[49] Khalafi-Nezhad, A. & Mohammadi, S. Highly efficient synthesis of 1-and 5-substituted 1 H-tetrazoles using chitosan derived magnetic ionic liquid as a recyclable biopolymer-supported catalyst. *RSC advances.* **3**, 4362-4371 (2013).

Figures

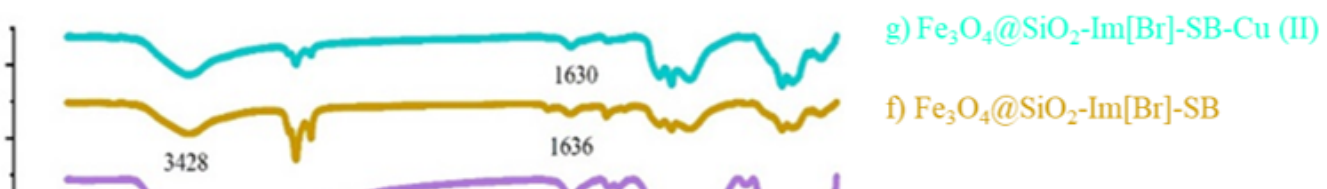


Figure 1

FT-IR spectra: a) Fe₃O₄; b) Fe₃O₄@SiO₂; c) Fe₃O₄@SiO₂-(CH₂)₃Cl; d) Fe₃O₄@SiO₂-Im; e) Fe₃O₄@SiO₂-Im[Br]; f) Fe₃O₄@SiO₂-Im[Br]-SB; g) Fe₃O₄@SiO₂-Im[Br]-SB-Cu (II)

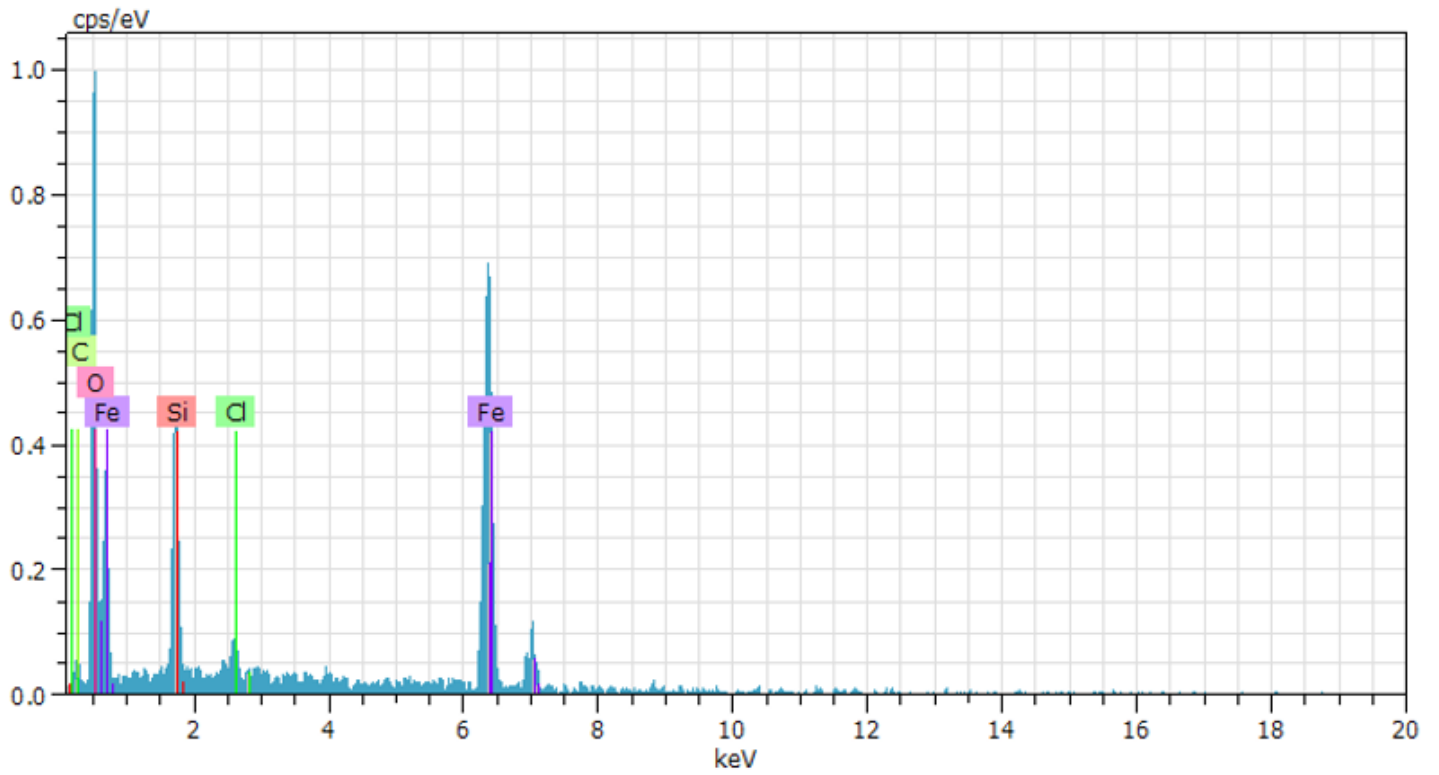


Figure 2

EDX Spectrum of $\text{Fe}_3\text{O}_4@\text{SiO}_2\text{-Cl}$

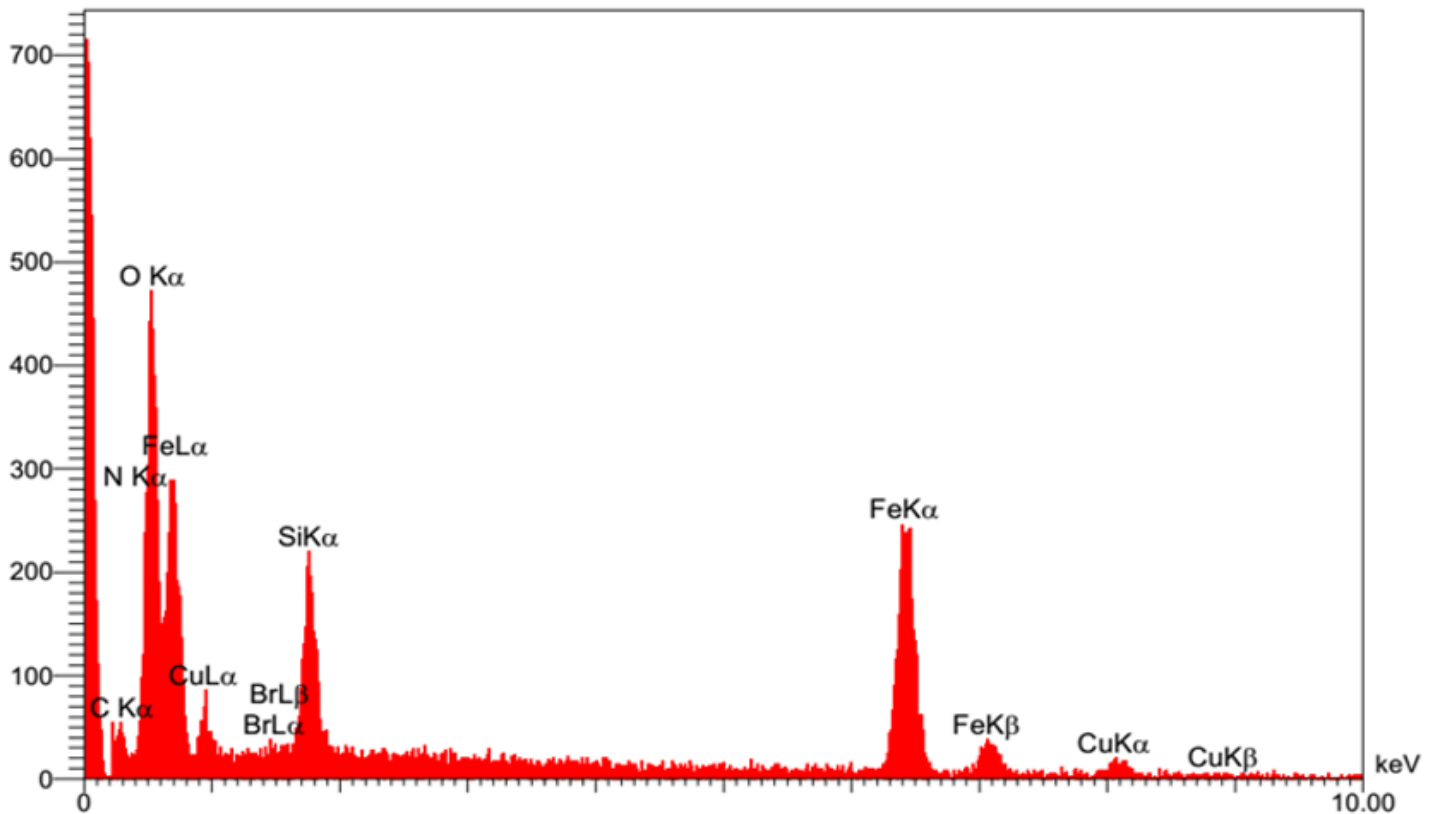


Figure 3

EDX Spectrum & data of $\text{Fe}_3\text{O}_4@\text{SiO}_2\text{-Im[Br]-SB-Cu (II)}$

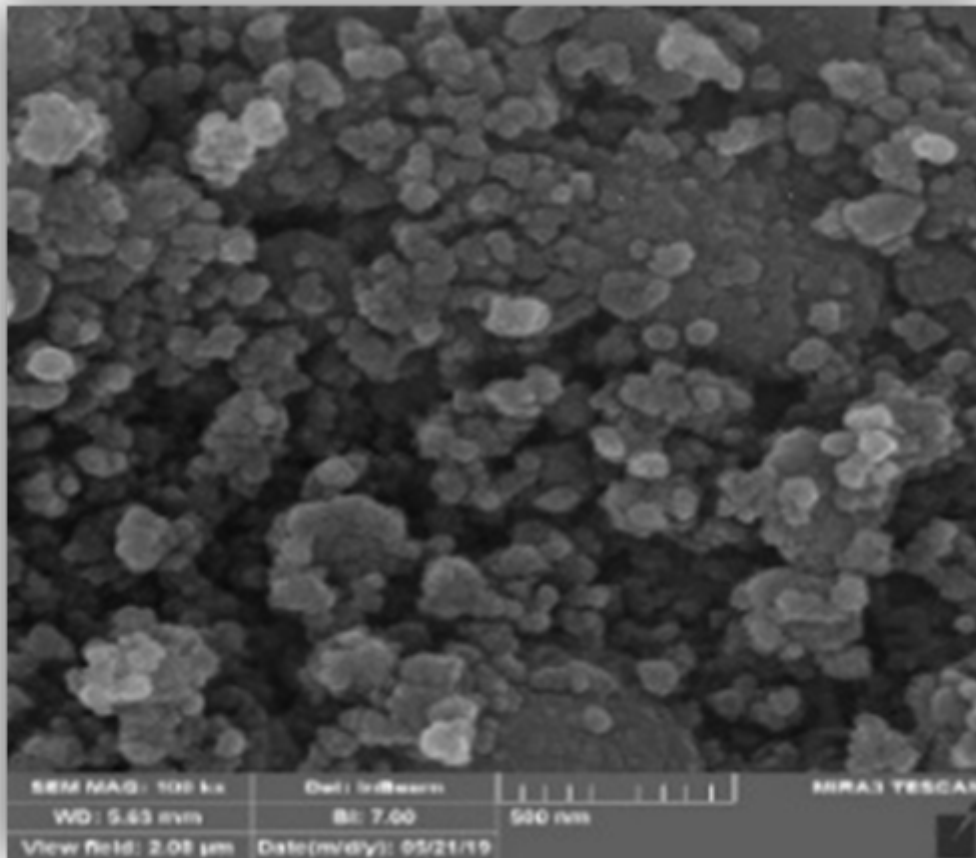


Figure 4

SEM image of $\text{Fe}_3\text{O}_4@\text{SiO}_2\text{-Im[Br]-SB-Cu (II)}$ nanocomplex

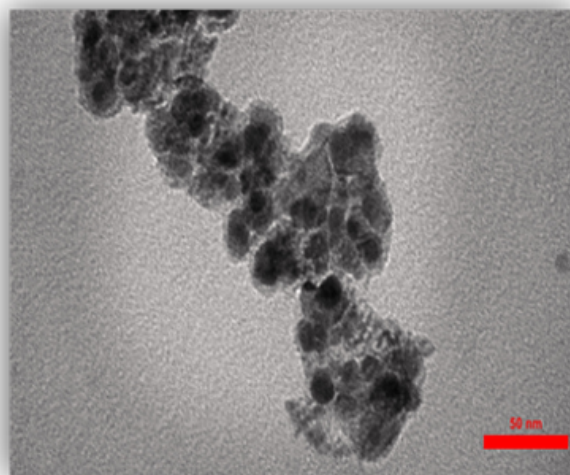
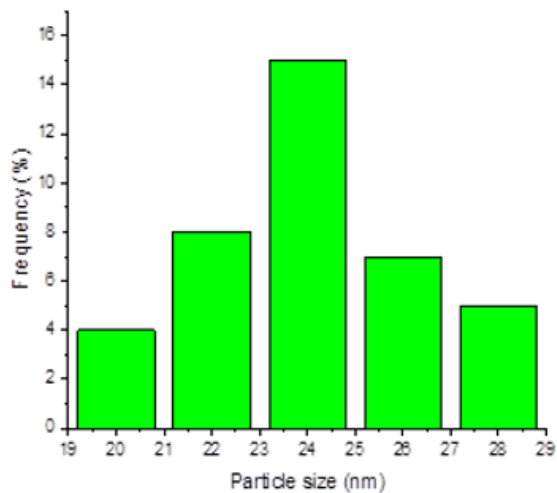


Figure 5

a) TEM image and b) histogram of $\text{Fe}_3\text{O}_4@SiO_2\text{-Im[Br]-SB-Cu(II)}$ nano complex

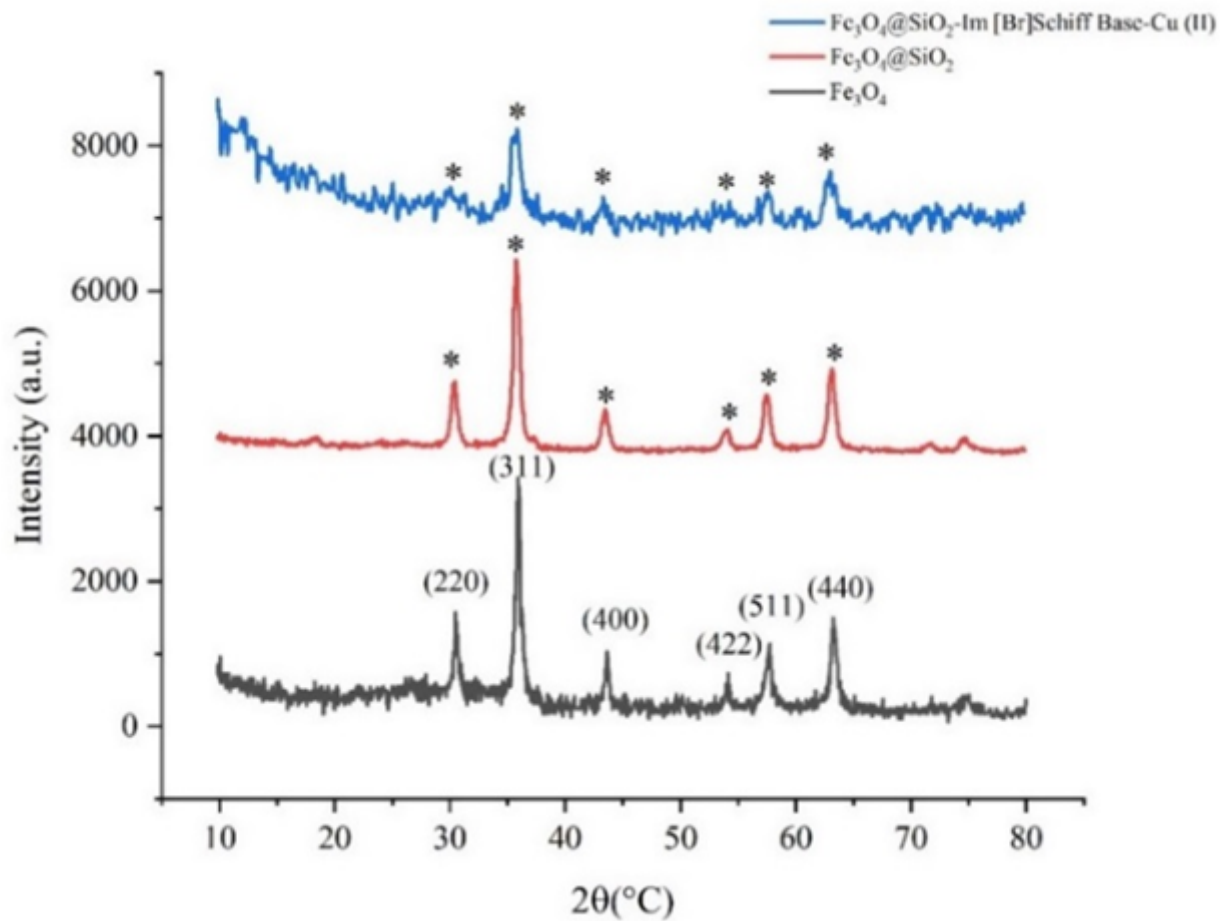


Figure 6

XRD patterns of Fe_3O_4 , $\text{Fe}_3\text{O}_4@\text{SiO}_2$ and $\text{Fe}_3\text{O}_4@\text{SiO}_2\text{-Im[Br]-SB-Cu (II)}$ nanocomplex

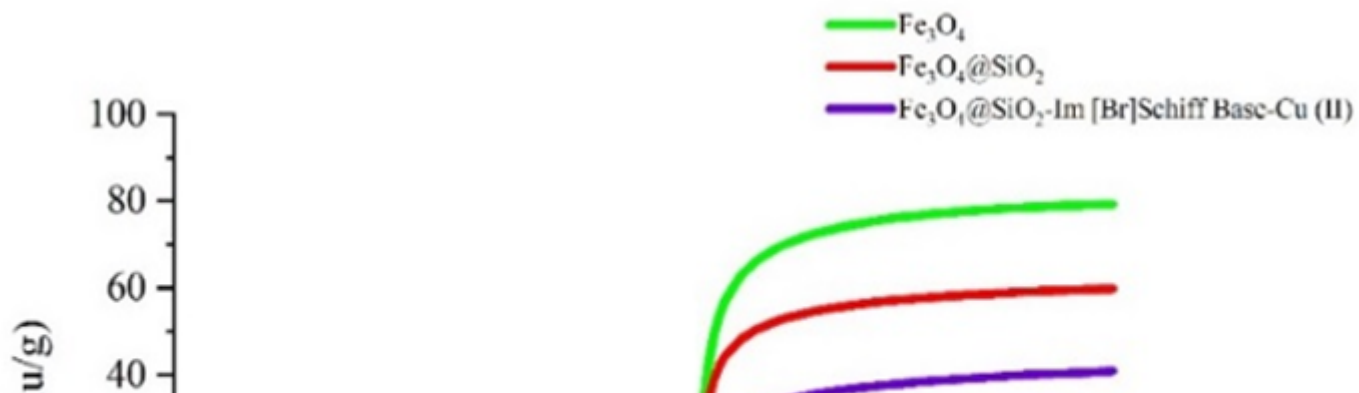


Figure 7

Magnetization curves of Fe_3O_4 , $\text{Fe}_3\text{O}_4@\text{SiO}_2$ and $\text{Fe}_3\text{O}_4@\text{SiO}_2\text{-Im[Br]-SB-Cu (II)}$ nano complex

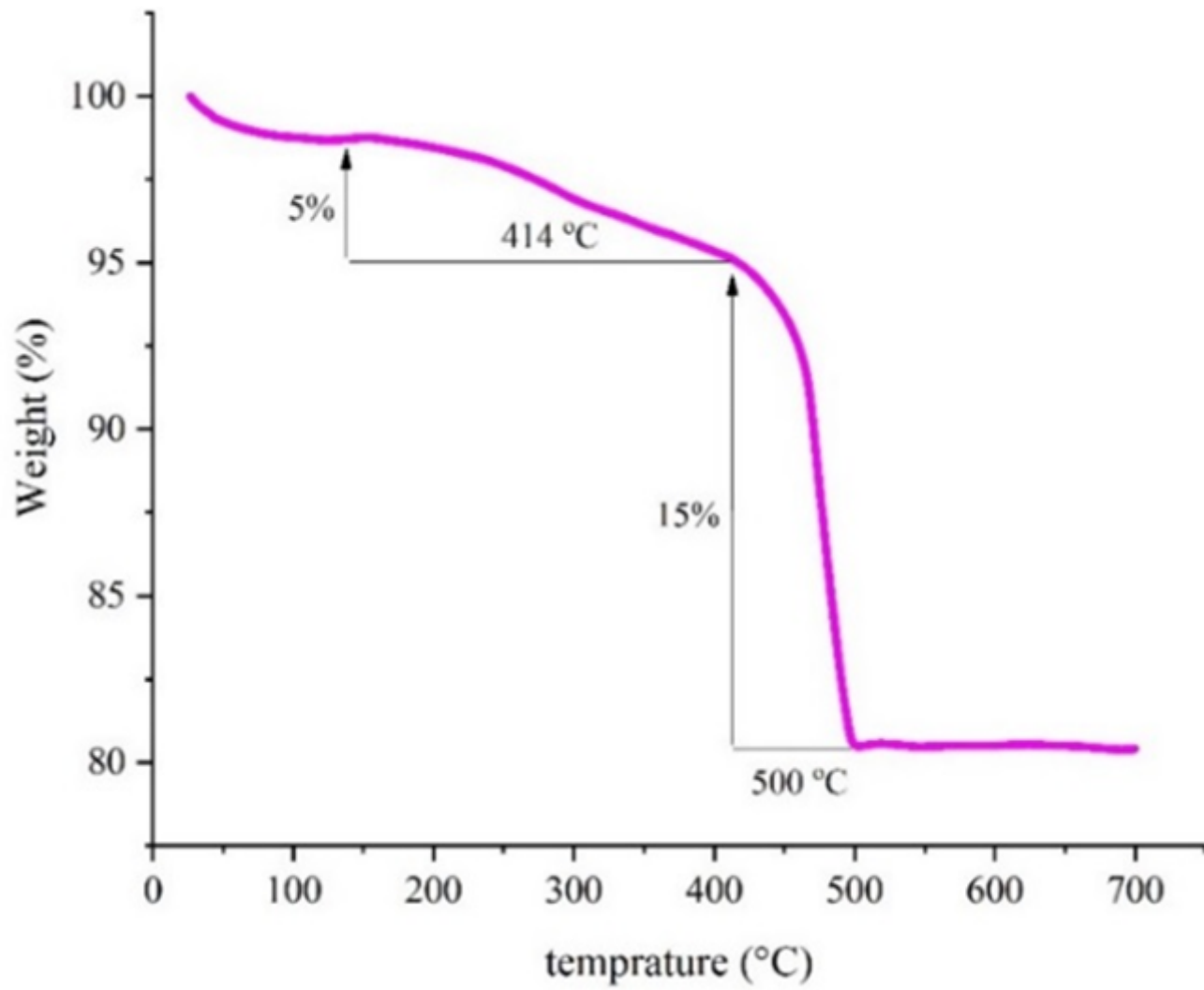


Figure 8

TGA of Fe₃O₄@SiO₂-Im[Br]-SB-Cu (II) nanocomplex

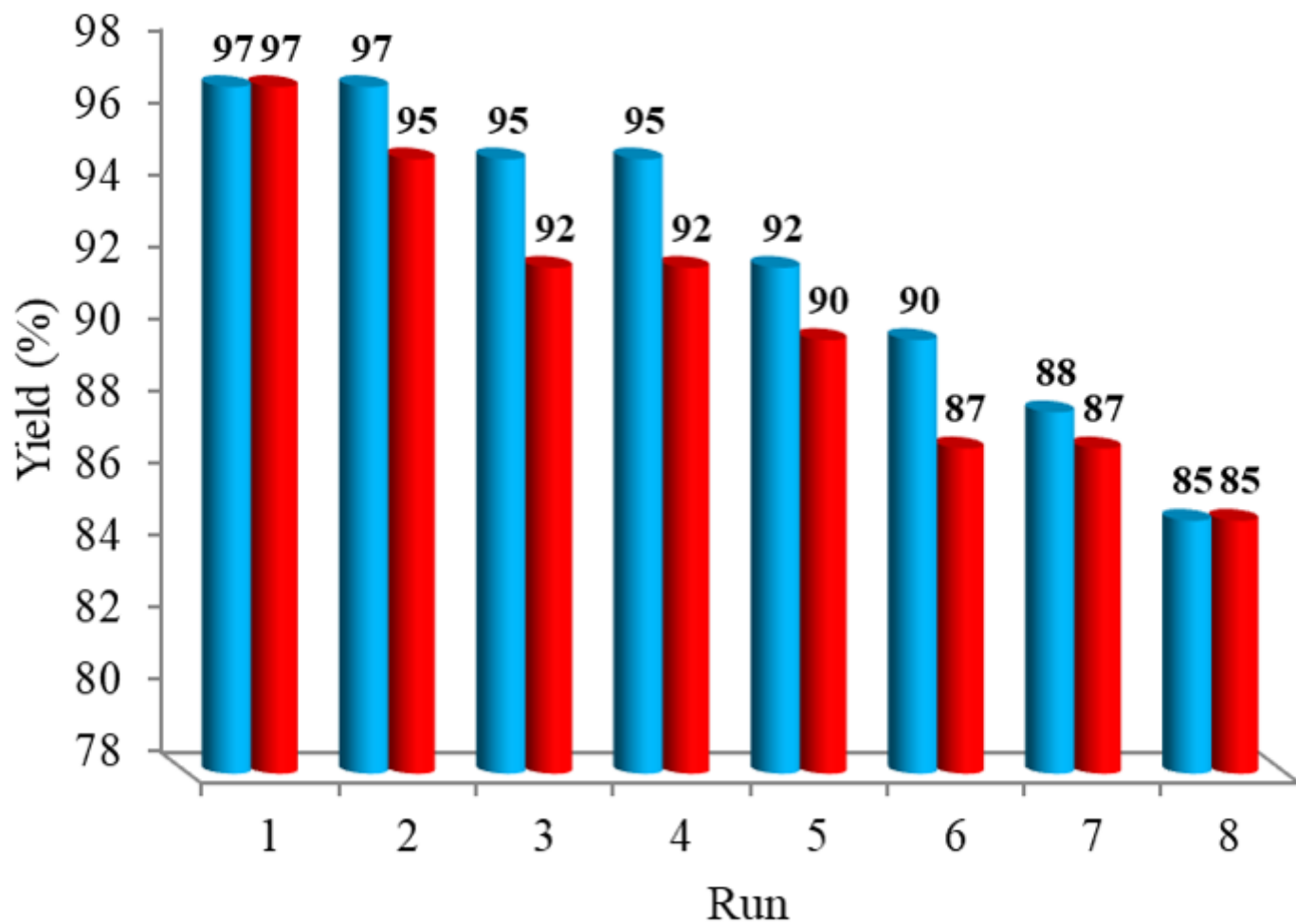


Figure 9

Recycling chart of $\text{Fe}_3\text{O}_4@\text{SiO}_2\text{-Im[Br]-SB-Cu(II)}$ MNP catalyst for the synthesis of 1-Phenyl-1H-tetrazole (blue) and 5-Phenyl-1H-tetrazole (red) derivatives

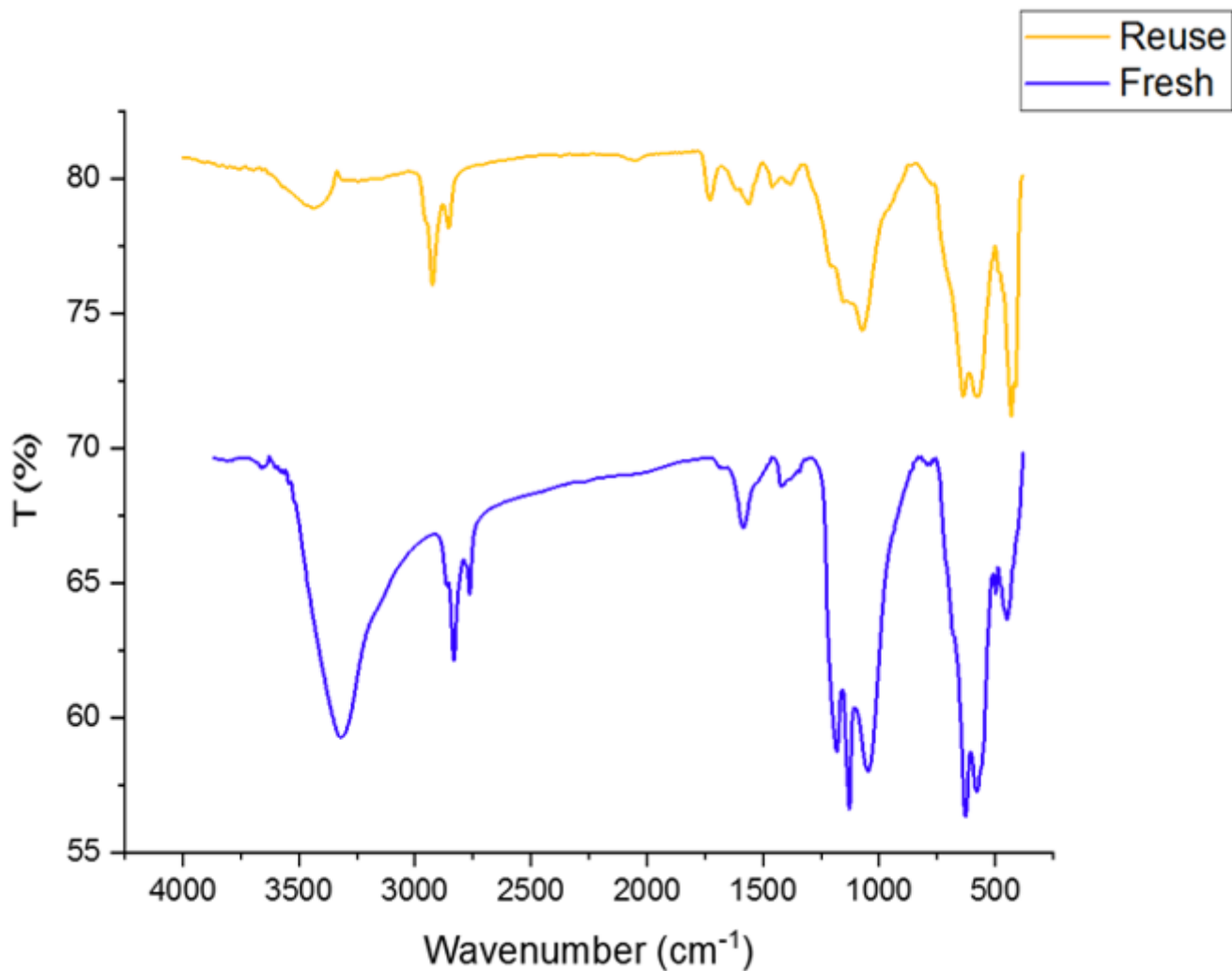


Figure 10

FT-IR spectra of fresh (blue) and reuse (orange) of $\text{Fe}_3\text{O}_4@\text{SiO}_2\text{-Im[Br]-SB-Cu(II)}$ MNP catalyst

Supplementary Files

This is a list of supplementary files associated with this preprint. Click to download.

- [scheme1.png](#)
- [scheme2.png](#)
- [scheme3.png](#)
- [scheme4.png](#)
- [scheme5.png](#)
- [SCHEME6.png](#)